INDONESIAN JOURNAL OF LIFE SCIENCES

RESEARCH ARTICLE

Check for updates

OPEN ACCESS

In Silico Evaluation of the Inhibition of *Pseudomonas aeruginosa* Biofilm Production in Burn Wound Infections Using CATH-2 and LL-37 Peptides

Priscilla Klaresza Adhiwijaya[1], Gabriella Zevania Kaitlyn[1], Louis Valenthenardo[1], Patricia Tiara Anjani[1], Mario Donald Bani[1]*

[1]*Department of Biotechnology, i3L University, Jakarta, Indonesia*

**Corresponding author: mario.bani@i3l.ac.id*

ARTICLE INFO

Article history:

Submitted January 17, 2025
Revised August 22, 2025
Accepted September 2, 2025

DOI: 10.54250/ijls.v7i02.238

KEYWORDS:

Biofilm inhibition, CATH-2, Lipopolysaccharides, LL-37, Pseudomonas aeruginosa

HIGHLIGHTS

- Burn wounds may often lead to sepsis due to the weakening of the skin's protective ability against biofilm-forming bacteria
- Binding cathelicidins, such as CATH-2 and LL-37, to LPS, may inhibit biofilm development in P. aeruginosa
- In silico, a comparison of the binding affinity of CATH-2 and LL-37 towards the three LPS—alginate, Pel, and Psl—reveals that CATH-2 can bind with the LPS stronger than LL-37 can

ABSTRACT

Patients with burn injuries are at high risk of bacterial infection due to the loss of the skin barrier, often leading to complications that contribute to increasing death tolls from burn injuries. The formation of biofilms in bacteria increases its survival rate, especially in the rise of antibiotic resistance cases, which ineffectively combats biofilm production. This research explores two natural antimicrobial peptides, LL-37 from humans and CATH2 from chickens. The study explores the potential of these peptides to defend against *Pseudomonas aeruginosa,* which is a major cause of infection in severe burn wounds, by blocking biofilm formation through its LPS region. *In silico* analyses were performed using AlphaFold, GLYCAM-Web, YASARA, and AutoDock Vina. It was found that the CATH-2 model has stronger binding affinities towards the three types of LPS—alginate, Pel, and Psl—scoring between -5.5 and -6.0 kcal/mol, as opposed to the score range of -4.3 to -6.0 for LL-37. These results suggest the encouragement of studying CATH-2 as a potential treatment against biofilm-protected *Pseudomonas aeruginosa* infection. In future studies, factors such as the safety and stability of the peptides must still be assessed and optimized in hopes of developing a product that can effectively reduce the high risks that severe burn wounds impose on patients.

INTRODUCTION

Severe burns, including deep second-, third-, and fourth-degree burn wounds, are often associated with high levels of mortality due to the pathogenicity that is caused. Such burns are caused by prolonged exposure to thermal energy from scalding materials or flames, which may eventually induce necrotic cell death across the different layers of the skin, extending farther than the most superficial epidermis (Radzikowska-Büchner et al., 2023). Unfortunately, these burn injuries rank as the fourth most common type of trauma (Greenhalgh, 2019). Due to their ability to rapidly degenerate tissues and even organs deep within the body, this disease causes more than 18 million disabilities, 7.1 million injuries, and 180,000 deaths every year (Wardhana et al., 2017; WHO, 2023). This is an especially-concerning issue in low- and middle-income countries, such as Indonesia, where more than 195,000 deaths were associated with burns in 2013 alone (Angkoso & Kekalih, 2022).

While several surgical interventions, such as excisions and skin grafts, may be done to promote the skin to repair itself; burn victims are still prone to complications throughout this long period of healing. Jeschke et al. (2020) mentioned that severe burn patients generally still have their mortalities significantly risked by complications even 5–10 years after their initial incident. This is because upon thermal damage, immediate dysfunction to the body's homeostasis and organ function occurs (Żwierełło et al., 2023). Additionally, with the skin as the body's first and largest defensive barrier is impaired, the body is left much more susceptible to internal infections from external pathogens (Burgess et al., 2022).

Among all burn-related deaths, sepsis is often found to be the leading cause, resulting in nearly 50% of patient loss, as opposed to hypovolemic shock (28%), renal failure (23%), and cardiac failure (1%) (Tasleem et al., 2024). This condition may lead to further threats of blood clotting, organ failure, and even death, caused by the persistent triggering of the body's immune system to eradicate virulent microorganisms circulating within the bloodstream (Gyawali et al., 2019). For this reason, the significance of antibiotic administration in burn patients has been highlighted. According to Soleymanzadeh-Moghadam et al. (2015), 40% of burn cases in Iran involved errors related to antibiotic prescription, dosage, or indication. Similarly, Aisyah et al. (2018) reported that 66.7% of the antibiotics used in burn patients were incorrectly-prescribed. These incidences have led to an increase in antibiotic resistance, as well as contributing to biofilm-associated infections and the disruption of the natural microbiome which requires an alternative approach to combat such conditions (Salam et al., 2023).

Hateet (2021) found that there are nine bacterial species commonly found in burn wounds. Among those, *Pseudomonas aeruginosa* has been found to be the most common bacteria present in burn wounds, making up an average of 20% of the bacterial population (Hateet, 2021). Burn wounds can secrete exudates that can promote the production of unique virulence factors in *P. aeruginosa*, such as pyocyanin and pyoverdine, which allow their rapid progression (Gonzalez et al., 2016). Furthermore, the ability of *P. aeruginosa* to form biofilms also acts as an additional issue in its eradication, as the accumulation of these structures can aid the survival of bacteria by promoting metabolic dormancy and antibiotic evasion (Ghosh et al., 2020; Preda & Săndulescu, 2019). This is especially an issue in burn wounds that can take up to months or years to fully heal, opening the need for long-term antibiotic use, which can lead to *P. aeruginosa*'s resistance to the mix of drugs (Dou et al., 2017; Jeschke et al., 2020). Therefore, an approach to address this issue is urgently needed to minimize the chances or duration of *P. aeruginosa* infection, such as by inhibiting its biofilm formation. While a variety of novel alternative treatments like quorum-sensing inhibitors, antimicrobial peptides, bacteriophage therapy, and antimicrobial photodynamic therapy have

begun to be developed, their safety and possible risk of developing resistant strains have not been studied enough to be utilized conventionally (Hughes & Webber, 2017).

One possible agent that has the prospect of being used as an inhibitor for biofilm formation in *P. aeruginosa* is the cathelicidin-2 peptide (CATH-2) (Scheenstra et al., 2019). In its active form, the peptide has been proven to kill microbes and trigger inflammation reactions by endogenous nucleic acid recognition (Kulkarni et al., 2021). Fortunately, CATH-2 is also known to be able to bind to lipopolysaccharides (LPS)—either alginate, pellicle (Pel), or polysaccharide synthesis locus (Psl)—which are an outer-membrane component of Gram-negative bacteria that play a role in initiating biofilm formation.

In *P. aeruginosa*, the O antigen outer-part of LPS is able to form bonds with lysine or arginine residues on histone-like (HU) proteins, embedding the bacterial cells into a polymer matrix and stabilizing the formation of biofilm (Huszczynski et al., 2020; Thakur et al., 2020). CATH-2 could compete for the negatively-charged binding site in LPS and this suggests that the addition of CATH-2 would prevent that interaction by destabilizing the biofilm scaffold but also neutralizes LPS-mediated immune evasion, shifting the balance toward bacterial clearance. This is also supported by a study done by Chen et al. (2018) that demonstrates the ability of CATH-2 to penetrate and eradicate *P. aeruginosa* within its biofilm by disrupting the biofilm matrix through direct interaction with extracellular polymeric substances (EPS, e.g., polysaccharides, extracellular DNA, and proteins) and inducing bacterial membrane permeabilization, leading to bacterial cell death.

CATH-2 is also produced by animals other than humans, including monkeys, rats, and chickens, to help the animal's defense against pathogens such as fungi, parasites, and gram-negative and gram-positive bacteria (van Harten et al., 2018). This is an indication that this compound may be obtained from widely available sources worldwide, possibly allowing the development of cheaper yet effective treatments for burn wound infections.

According to Ridyard and Overhage (2021), there is another peptide that belongs to the CAMP group called LL-37, which has antimicrobial activity, immunomodulation effect, and can help promote wound healing by potentially eradicating biofilm formation in *P. aeruginosa*. The main difference between the two peptides lies in their amino acid chains and structure. CATH-2 has 154 amino acids and LL-37 has 37, but as members of the same family, the two can participate in comparable pathways and functions (Scheenstra et al., 2020).

Through this research, a comparison of the binding strength of CATH-2 and LL-37 towards the three types of LPS was assessed. It is hoped that the acquired data may help future research in developing the possibility of using these peptides as potential treatment for biofilm-protected *P. aeruginosa* infection, especially in high-risk burn patients.

MATERIALS AND METHODS

Characterization of CATH-2, LL-37, and LPS

The amino acid sequence for CATH-2 was first sourced from Uniprot (https://www.uniprot.org/), where CATH-2 is listed by the accession number Q2IAL7. As CATH-2 does not have an established structure available in online databases, AlphaFold (https://alphafold.ebi.ac.uk/) was used to generate its 3D structure based on its amino acid composition and predicted folding patterns by inputting the peptide's amino acid sequence into its search bar. Meanwhile, the structure for LL-37 was obtained from the Research Collaboratory for Structural Bioinformatics Protein Data Bank (RCSB PDB, https://www.rcsb.org/), where it is denoted by the identification code 2K6O. However, since LPS are not proteins, their structures could not be

found or generated in any of the aforementioned tools, hence their 3D configurations were built using GLYCAM-Web (https://glycam.org/).

3D structure visualization

The 3D configurations of CATH-2, LL-37, and the three LPS were all visualized with the software Yet Another Scientific Artificial Reality Application version 23.5.19 (YASARA, https://www.yasara.org). YASARA is powered by a portable vector language (PVL), allowing it to visualize larger proteins and real-time interactions more accurately (Pradhan & Sharma, 2014). YASARA also allows easier manual selection and coloring of amino acid residues to mark key components of the protein. However, in this case YASARA was mostly used for a preliminary closer inspection of the molecules and the separation of the different models into separate PDB files. These generated structures were further processed in Autodock Vina to generate the molecular docking and interaction sites.

Simulation of molecular docking and identification of interaction sites

To predict the binding affinity of CATH-2 and LL-37 towards LPS, molecular docking was performed using AutoDockVina v1.5.7 (https://vina.scripps.edu/) for input preparation. This software was selected because of its hybrid empirical and knowledge-based scoring function, which has been shown to be both accurate and efficient compared to earlier AutoDock versions and related programs (Sarkar et al., 2023). The 3D structures of the two ligands, LL-37 and CATH-2, were first energy-minimized. The LPS receptor models, consisting of O antigen and its saccharides, were prepared at physiological pH with deprotonated phosphate groups, followed by hydrogen addition, Gasteiger charge assignment, and conversion to PDBQT format. Peptides were defined as flexible ligands, whereas the O antigen was treated as rigid. Binding sites were identified by an initial blind docking across the LPS surface, with poses clustered by binding energy and spatial overlap; the most populated cluster localized to the O antigen headgroup, where refined docking was subsequently performed. Each peptide was docked in ten independent replicates with exhaustiveness set to 32, generating up to 20 binding modes within 3 kcal/mol. Predicted complexes were evaluated by binding affinity, cluster stability, and key interactions (salt bridges, hydrogen bonds, hydrophobic contacts). Validation included redocking of a known LPS-binding peptide, scrambled peptide controls, and sensitivity analyses with varied docking parameters.

RESULTS

3D structure visualization

Four separate models of LL-37 structure taken from the same angle in YASARA are shown in **Figure 1**. The different variants remain the same in amino acid sequence, but differ slightly in conformation. The AlphaFold-predicted structure of CATH-2 and its subsequent visualization in YASARA can be seen below in **Figure 2.**

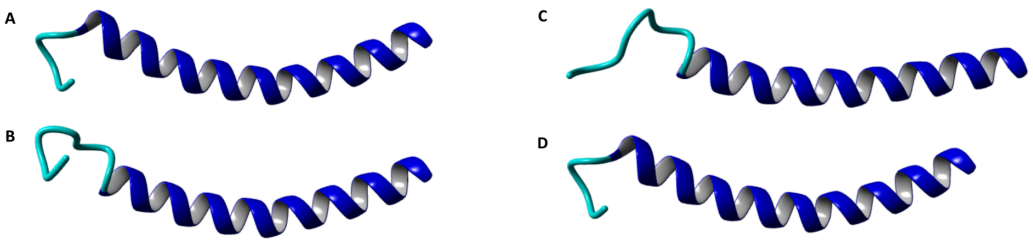

Figure 1. 3D visualization of four LL-37 peptide models taken from the same angle with YASARA. Henceforth, the poses are recognized as LL-37 Model 1 (**A**), Model 2 (**B**), Model 3 (**C**), and Model 4 (**D**)

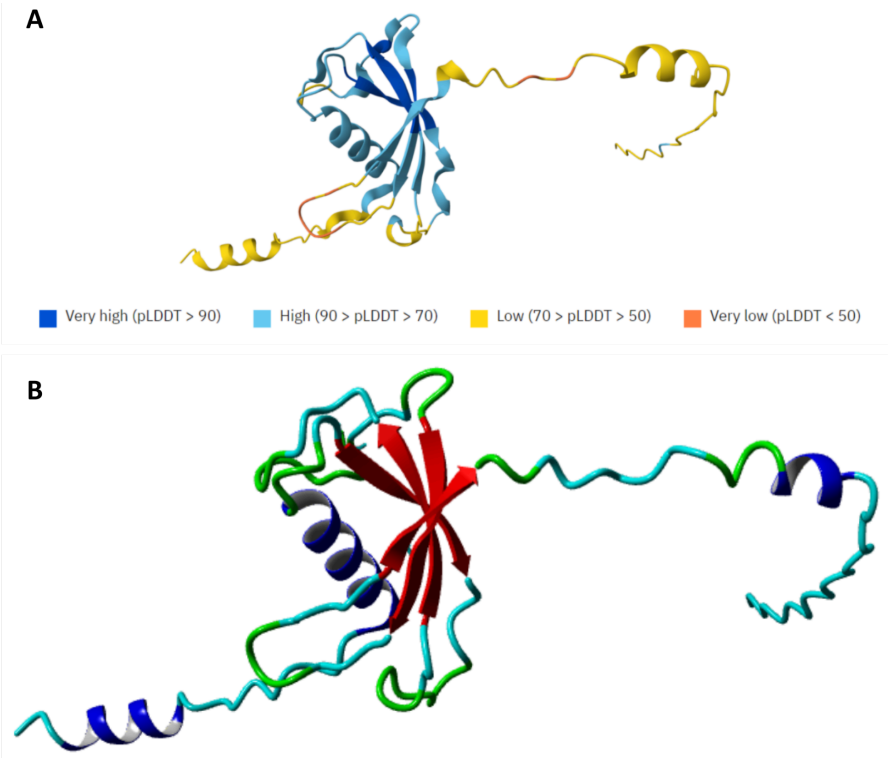

Figure 2. Predicted structure of CATH-2 with model confidence indicators from AlphaFold (**A**) and 3D visualization of CATH-2 peptide with YASARA (**B**)

Figure 2A shows that AlphaFold predicted the 3D structure for CATH-2 with varying levels of confidence across its amino acid sequence (further elaborated in supplementary material **Table S1**). The protein structure is categorized into parts predicted with either very high, high, low, or very low confidence. It can be observed that segments towards the middle of the protein tend to be predicted with higher confidence, while those along the outside edges of the protein with lower confidence. **Figure 2B** shows the successful transfer of the entire AlphaFold-predicted structure for CATH-2 as a PDB file for further processing in AutoDock Vina.

The 3D structures for the three LPS can then be seen below in **Figure 3**.

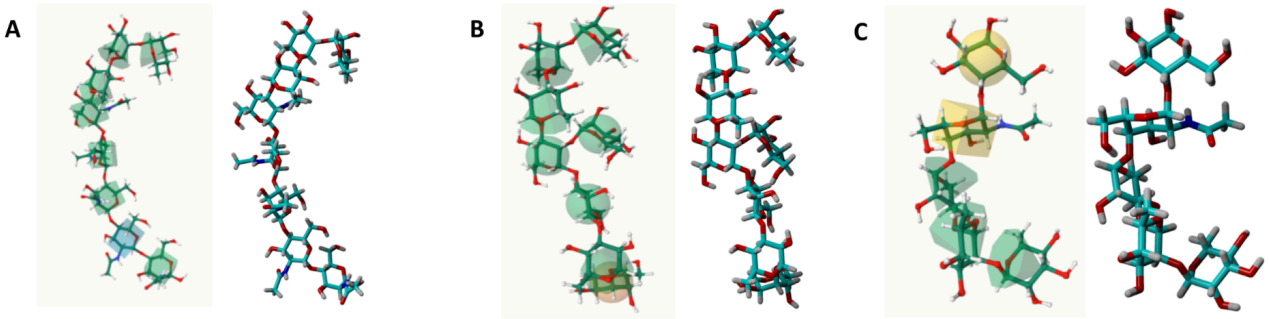

Figure 3. 3D visualization of alginate LPS (**A**), PsI LPS (**B**), and PeI LPS (**C**) with GLYCAM-Web (left) and YASARA (right)

Simulation of molecular docking and identification of interaction sites

To evaluate the binding affinity and evaluate the amino acid residues that interact between CATH-2 and LPS, molecular docking was performed with AutoDockVina. The potential affinities and interacting amino acids between CATH-2 and alginate, Pel and Psl, can be found below in **Table 1**.

Table 1. Potential affinities and interacting amino acid residues of CATH-2 towards the three LPS

Protein	LPS	Affinity (kcal/mol)	Interacting amino acid residues
CATH-2	Alginate	-5.5	ILE 94, THR 69, ASN 67, SER 95, ASP 51, LEU 53, THR 62, ARG 64
	Pel	-6.0	PRO 19, ALA 20, ASP 106, LEU 22, VAL 103, GLN 30, GLN 26, ASP 33, GLN 37
	Psl	-6.0	ASP 34, ARG 46, LEU 47, ILE 29, PRO 25, TYR 24, GLU 53, ALA 50, SER 49

Table 1 shows that CATH-2 would most likely be attracted to the three LPS with different affinities, namely -5.5 kcal/mol with alginate and -6.0 kcal/mol with both Pel and Psl, indicating a slightly stronger binding with the latter two. The table also details the amino acids of CATH-2 that would interact with each respective LPS to facilitate the binding. Meanwhile, **Table 2** below shows the potential affinities and interacting amino acids between four models of LL-37 and alginate, Pel, and Psl.

Table 2. Potential affinities and interacting amino acid residues of the four LL-37 models towards the three LPS

Protein	LPS	Affinity (kcal/mol)	Interacting amino acid residues
LL-37 Model 1	Alginate	-5.3	GLU 11, LYS 15, LYS 18, GLN 22, ARG 19, ARG 23
	Pel	-5.0	ASN 30, ARG 23, ARG 19, PHE 27, ASP 26
	Psl	-4.6	ARG 23, ASP 26, LYS 25, GLN 22, LYS 18, ARG 19
LL-37 Model 2	Alginate	-4.9	SER 37, GLU 36, ASN 30, ASP 26, ARG 23, GLN 22, ARG 19
	Pel	-4.7	SER 37, PRO 33, GLU 36, ASN 30, ARG 23
	Psl	-6.0	GLU 36, ASN 30, ARG 23, ASP 26, ARG 29, GLN 22, LYS 25, ARG 19
LL-37 Model 3	Alginate	-4.6	THR 35, LEU 31, ASN 30, ARG 29, ARG 23, GLN 22, ARG 19
	Pel	-4.3	ASN 30, PHE 27, ARG 23, ILE 20
	Psl	-4.6	THR 35, VAL 32, ASN 30, ARG 29, ASP 26
LL-37 Model 4	Alginate	-5.2	ASN 30, PHE 27, ARG 23, ILE 20, GLN 22, ARG 19, LYS 15
	Pel	-5.0	ASN 30, PHE 27, SER 37, ARG 29, ASP 26, ARG 23
	Psl	-5.1	PRO 33, SER 37, ASN 30, PHE 27, ARG 23

As seen in **Table 2**, each analyzed interaction between the LL-37 models and the three LPS also involves different degrees of binding affinity, ranging from -4.3 to -6.0 kcal/mol. The table also lists the interaction sites that facilitate each binding.

In accordance with the interacting amino acids listed in **Table 1**, the interaction sites of the CATH-2 and the three LPS are visualized in a 3D space below in **Figure 4**.

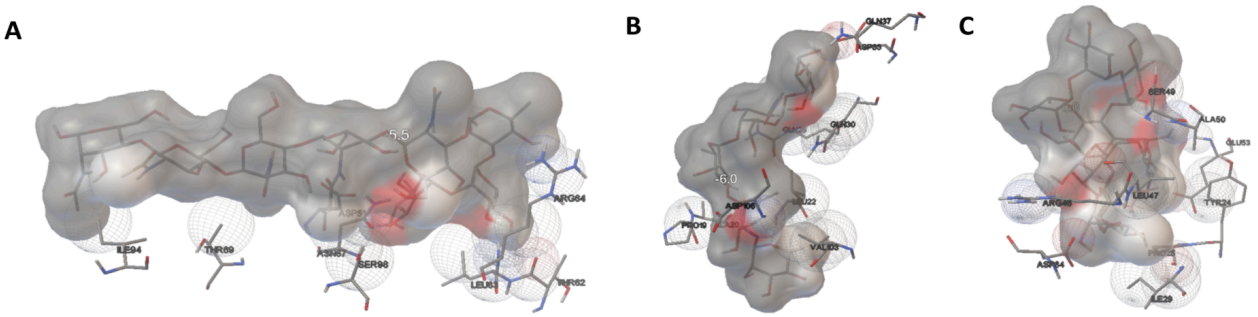

Figure 4. 3D visualization of the interaction sites of CATH-2 with alginate (**A**), Pel (**B**), and Psl (**C**)

Figure 4 depicts the three LPS as gray structures, while the interacting amino acids of CATH-2 were positioned where it would bind with the LPS.

The interaction sites of the four LL-37 models and the three LPS can then be seen in **Figure 5** below.

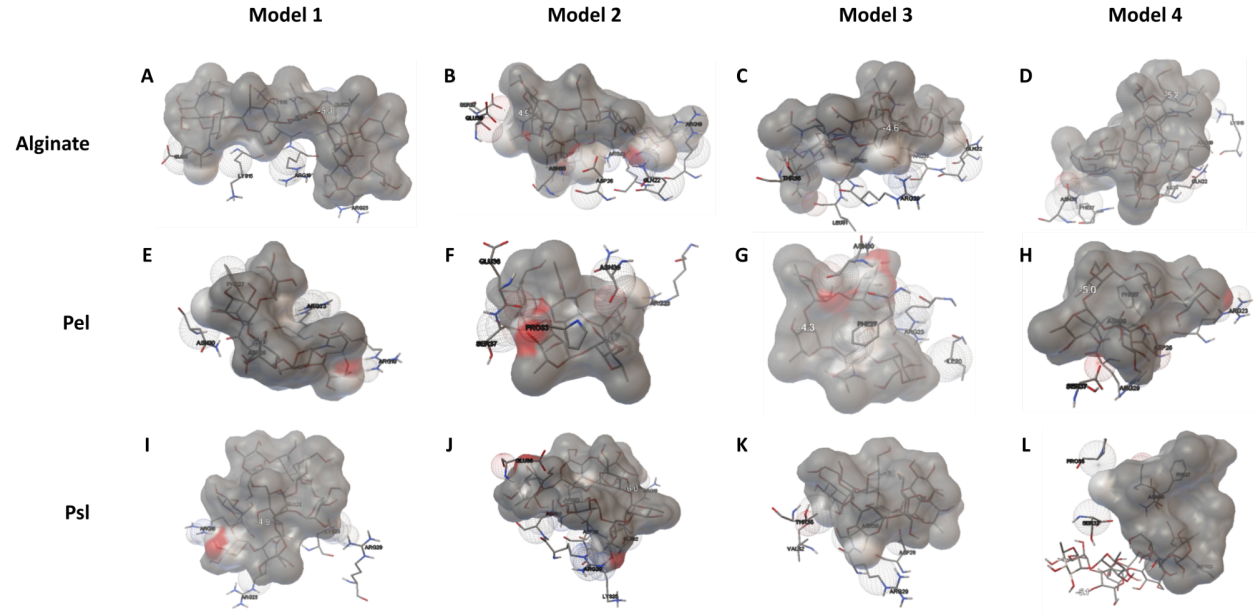

Figure 5. 3D visualization of the interaction sites of LL-37 Models 1–4 with alginate (**A–D**), Pel (**E–H**), and Psl (**I–L**)

Likewise, **Figure 5** shows the LPS as gray structures and the interacting amino acids of LL-37 were placed where they would bind with the LPS.

DISCUSSION

Characterization of CATH-2, LL-37, and LPS

LPS, which resides on the outer membrane of gram-negative bacteria, acts as a defense mechanism. LPS give the bacteria structural integrity and a permeability barrier to prevent harmful chemicals from

interacting with their metabolism. LPS also induces the development of persistent biofilm that hinders wound treatments (Farhana & Khan, 2023). It was suggested that binding specific inhibitory molecules, such as cathelicidins (CATHs), to the LPS may prevent this mechanism.

CATHs are host defense peptides with immunomodulatory and antimicrobial functions, exhibiting strong activity against a variety of bacteria, parasites, and fungi (van Harten et al., 2018). Although approximately 30 different CATHs have been identified across species, this study focuses on LL-37, the only cathelicidin found in humans, and CATH-2, one of the cathelicidins present in chickens (Schneider et al., 2016). These two peptides were selected due to their well-characterized antimicrobial and immunomodulatory properties, as well as their relevance to human and avian biology, which makes them suitable candidates for translational studies.

Both LL-37 and CATH-2 prevent *P. aeruginosa* biofilm formation by impairing bacterial motility, reducing adhesion, and downregulating the transcription of Las and Rhl, genes that controls the virulence factor, biofilm formation, and quorum-sensing systems (Xiao et al., 2022; Yasir et al., 2018). Additionally, these peptides disrupt the extracellular polymeric matrix of biofilms through degradation, release of membrane lipids, and bacterial detachment, ultimately inhibiting biofilm formation. These effects are thought to occur via electrostatic interactions, where the positively charged peptides disrupt the negatively charged LPS structures, interfering with their normal function (Varela et al., 2021).

3D structure visualization

The structure of LL-37 in YASARA can be seen as four separate models in **Figure 1**. The four were reported to be conformers, meaning that all four were made from the same number and sequence of amino acids, but differ in the rotation of at least one bond (Zhang et al., 2022). These rotational variations can be seen throughout the helical portion of the four structures, but are especially-evident in their C-terminal tails starting from VAL 32. The finding of these LL-37 structures were acquired with solution NMR, but did not provide further information on which conformer is deemed to be the most accurate for *in silico* analyses (Wang, 2008). Therefore, all four were used in this study.

A PDB file for CATH-2 could not be found, meaning a verified 3D structure for the protein has not been uploaded to the database for use. To mitigate this, AlphaFold was used to predict a structure that could be translated into a PDB file, which yielded the image shown in **Figure 2A** from AlphaFold and **Figure 2B** in YASARA. As summarized in **Table S1**, interpreting the structure would reveal that only 15 amino acids received a confidence rating of very high predicted Local Distance Difference Test (pLDDT > 90), 59 amino acids were high (90 > pLDDT > 70), 73 amino acids were low (50 > pLDDT > 50), and 7 amino acids were very low (pLDDT < 50). The pLDDT is a parameter measuring residue-by-residue credibility based on the Local Distance Difference Test Cα (LDDT-Cα) metric (Varadi et al., 2022). On this scale, amino acids rated with low and very low confidence are more likely to be less accurate in their actual form. Therefore, it cannot be assumed to be absolutely correct. Such low confidence levels would typically align with disordered regions within the protein being analyzed, which are segments possessing very unstable foldability due to frequently changing molecular forces (Bondos et al., 2022; Ruff & Pappu, 2021).

According to Chung et al. (2023), the involvement of the three types of LPS in biofilm formation and maintenance heavily depends on the strain of bacteria that produces it. For instance, in *P. aeruginosa* strain PAO1, Psl significantly contributes more to the construction of the bacterium's biofilm matrix, while the highly virulent strain PA14 relies more on Pel. Therefore, all three LPS were assessed for their binding strengths with CATH-2 and LL-37 in this study.

Since LPS are not proteins that can be found in the RCSB Protein Data Bank, rather molecules with lipid and saccharide constituents, it was required to be built from scratch. Unfortunately, the entire structure of the three LPS is still not exactly known. However, several studies, such as those by Franklin et al. (2011) and Melamed & Brockhausen (2021), have provided findings as to their possible appearance. In particular, it is known that the general structure of LPS, as shown in **Figure 6**, consists of an O antigen, outer core, inner core, and a membrane-anchored lipid A. It is also known that O antigens differ among species and strains, acting as an identifiable marker, and that the three LPS mainly differ in the sequence of glycans that make up their inner and outer core (Melamed & Brockhausen, 2021).

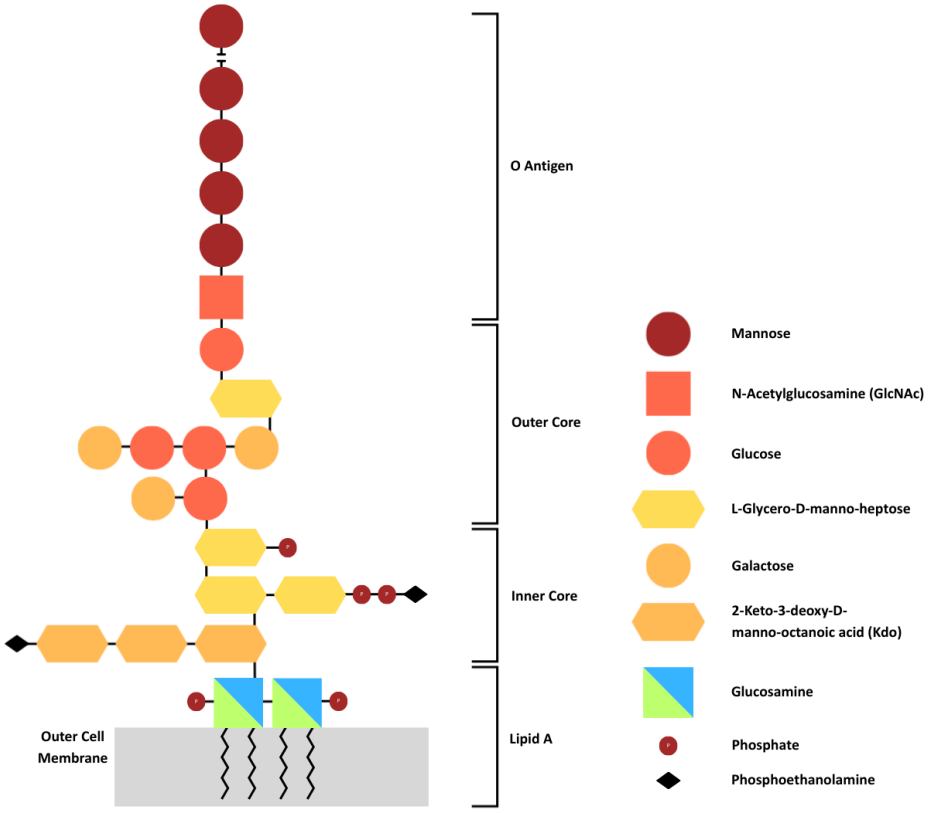

Figure 6. The general structure of LPS

Using the current knowledge of LPS structures as a guide, the structures in **Figure 3** were made using GLYCAM-Web and subsequently visualized in YASARA. The translucent spheres on peptide structures indicate potential binding sites for target molecules. Each color represents a distinct chemical environment, where green spheres typically mark polar regions, which are most favorable for binding due to their ability to form hydrogen bonds. These zones are often dominant in LPS, suggesting a high likelihood of interaction. Blue spheres highlight electropositive zones, commonly enriched with basic residues like lysine and arginine, which can engage in electrostatic interactions with negatively charged groups on the target. Lastly, yellow spheres denote hydrophobic regions, which are usually buried and less accessible, making them less likely to participate in binding.

Simulation of molecular docking and identification of interaction sites

AutoDock Vina was used to evaluate the binding strengths of the two peptides towards the three LPS structures by showing their affinity scores and interacting amino acid residues. The binding affinity

value depicts the strength of the interaction between the protein and LPS, in which a more-negative affinity score indicates a stronger and more stable interaction in the binding site due to higher energy release (Cabral et al., 2022). From all the results generated, the poses with the lowest root-mean-square deviations (RMSD) values were used. As RMSD is a measure of the difference in position between the predicted conformation and the reference structures, choosing a docking scenario with the lowest possible RMSD value should ensure optimal precision among the other generated poses (Vittorio et al., 2024). Fortunately, in all models, a pose with an RMSD near 0 Å was observed. This indicates that the predicted poses had high precision.

The results in **Tables 1** and **2** showed that the strongest affinity was generated from the binding of CATH-2 with all the LPS where the respected acquired values for alginate, Pel, and Psl were -5.5 kcal/mol, -6.0 kcal/mol, and -6.0 kcal/mol respectively. LL-37 has four models based on its PDB structure. After each model was tested for binding with each LPS, it was found that LL-37 Model 1 has the best binding affinity with alginate, with a score of -5.3 kcal/mol. Models 1 and 4 were found to have the same affinity score of -5.0 kcal/mol when bound to Pel. Model 2 has the strongest affinity of -6.0 kcal/mol bound with Psl, while Model 3 has the lowest binding affinity towards each LPS.

While there has not been an established criterion on the range of affinity values that can be considered weak or strong, several papers can be used as reference when making such judgements. For instance, Alsedfy et al. (2024) mentions -7.0 kcal/mol to be the ideal threshold, while Lin et al. (2025), and others state that -5.0 kcal/mol is enough to be considered favorable. Using the latter as a standard, only the affinities of LL-37 Model 4 and CATH-2 can be considered to be strong against all three LPS, with CATH-2 showing stronger affinities overall.

It is possible that the peptides analyzed can still have their binding affinities with the three LPS optimized by engineering them to only include critical binding sites. This is because the longer and more complex a protein is, the more chances that factors such as steric hindrance and charges may inhibit effective binding (Muntaha et al., 2025). While **Tables 1** and **2** show the list of amino acid residues involved in the receptor-ligand binding, having 3D maps of each interaction site may greatly help future studies in understanding which parts of the peptides are encouraged to be focused on. The interaction sites of CATH-2 and the three LPS can be seen in **Figure 4** and **5**.

In **Figure 4** and **5**, LPS is represented by the translucent gray structure. Meanwhile the scattered smaller structures indicate the possible binding sites of the peptide ligand. For instance, **Figure 4A** depicts the binding of CATH-2 with alginate, which has a binding affinity of -5.5 kcal/mol, and the possible interacting residues of ILE 94, THR 69, ASN 67, SER 95, ASP 51, LEU 53, THR 62, and ARG 64. Visualization of the binding of these sites in 3D space may help future research in optimizing the effectiveness of these peptides against LPS.

CATH-2 and LL-37, are antimicrobial peptides from the cathelicidin family that can inhibit biofilm formation through multiple strategies (Dzurová et al., 2024). Their positive charge and unique structure allow them to attach to the negatively charged surfaces of bacterial cells, leading to membrane disruption, pore formation, and bacterial death before the cells can settle and initiate biofilm formation (Sancho-Vaello et al., 2020; Sharma et al., 2023). These peptides can also prevent bacterial attachment to surfaces by binding to adhesin proteins, altering cell surface charges, or masking receptor sites on host cells that bacteria typically target (Keikhosravani et al., 2023; Ridyard & Overhage, 2021).

In addition, these peptides also disrupt quorum sensing. This is the chemical communication system bacteria use to coordinate biofilm development by downregulating key genes responsible for producing and detecting signaling molecules such as lasI, lasR, rhlI, and rhlR (Xiao et al., 2022). Beyond their direct

antimicrobial effects, CATH-2 and LL-37 enhance the host's immune defense by attracting and activating immune cells such as neutrophils and macrophages. These peptides also modulate cytokine production to create an environment less favorable for bacterial survival (Duarte-Mata & Salinas-Carmona, 2023). By combining these actions, both CATH-2 and LL-37 are able to prevent attachment, interfere with bacterial communication, cause breakdown of biofilm structure, and activation of the immune system. Moreover, CATH-2 and LL-37 also act as potent inhibitors of biofilm formation (Keikhosravani et al., 2023; Ridyard & Overhage, 2021). Hence, both peptides remain promising candidates for future *in vitro* or *in vivo* studies. While the results were derived from *in silico* research, the findings may contribute to developing revolutionary treatments for burn wound patients.

Nonetheless, various limitations in this research must still be considered for future optimization or related research. One limitation of the method used was the inability of GLYCAM-Web to insert any acetyl or lipid groups. Fortunately, many studies, such as one done by Whitfield et al. (2020) have shown that the lipid constituent of the LPS are unlikely to be the part responsible for binding with the cathelicidins. Rather, the O antigen has a higher chance of playing this role. This binding possibility becomes a limitation that may hinder the accuracy of the docking results.

In addition, this research did not include any positive or negative control. The main objective of this study was solely to compare which of the two cathelicidins speculated are able to inhibit biofilm formation by forming stronger bonds with the three LPS.

Another limitation is the usage of an AlphaFold-predicted 3D structure for CATH-2 due to the lack of an established PDB structure from wet lab experiments. AI-predicted structures may still lack accuracy to its real-life counterpart, as it only relies on the typical principles of protein folding. The prediction can fail in emulating the dynamics of existing charges, ligands, and other environmental factors (Terwilliger et al., 2024). However, we have ensured to use the structure labeled as “reviewed” and “reference proteome”, which means that it has been approved and featured by the protein database UniProt. The resulting structure was still predicted with varying degrees of confidence, as seen in **Figure 2**. In other cases, a structure prediction tool that is more specific for the prediction of peptides, such as PepFold, would have been preferable. However, PepFold was unfortunately unavailable for use due to maintenance at the time of this study.

Our findings only indicate which ligand is more likely to bind strongly to LPS. It does not provide any information on the actual therapeutic effectiveness of the peptides. Thus, much further testing is still required to establish the safety and efficacy of such treatments through *in vitro* or *in vivo* studies.

Further research into product development should also be conducted. While peptides have now been incorporated into various skincare formulations, such as topical creams and solutions, neither CATH-2 nor LL-37 have been assimilated into the conventional market. There is a need to carefully study the stability and penetrative abilities of the peptides to create an effective product (Al Musaimi et al., 2022).

Alternatively, one possible method of directly facilitating the production of CATH-2 or LL-37 within burn wounds is by utilizing genetically engineered *Staphylococcus epidermidis*, which is a common bacterium that live in symbiosis on the human skin, where inserting a CATH-2 or LL-37-encoding plasmid into this bacterium may facilitate the safe expression of the peptide (Lee & Anjum, 2023).

CONCLUSION

Severe burn wounds are often associated with high mortality, where an estimated 180,000 annual deaths arise across the world. Among its complications, sepsis due to virulent microorganism circulation in the bloodstream accounts for around half of patient losses. Antibiotic treatment is slowed down further

when common burn wound bacteria, such as *P. aeruginosa,* forms biofilm. This increases risks of antibiotic resistance. Thus, to prevent biofilm formation, inhibitory peptides like CATH-2 and LL-37 may be employed to bind with biofilm-forming LPS.

Several models of CATH-2 and LL-37 were tested for their affinities towards the three types of LPS using AutoDock Vina. CATH-2 scored affinity values between -5.5 and -6.0 kcal/mol, while LL-7 scored between -4.3 to -6.0. While the two ranges are similar, it is suggested that CATH-2 would have a higher overall chance of binding stronger to the three LPS. Unfortunately, this study does not adequately consider the effectiveness, safety, or stability of the peptides as a potential treatment plan. Such matters must continue to be assessed through further research, product development, and clinical trials to achieve a reliable conclusion. As biofilm-protected *P. aeruginosa* infection continues to impose significant risks onto burn patients, it is hoped that further exploration into the potential of cathelicidins, especially CATH-2, to treat this issue may continue to advance.

SUPPLEMENTARY MATERIALS

Table S1. Validation of AlphaFold prediction

REFERENCES

Al Musaimi, O., Lombardi, L., Williams, D. R., & Albericio, F. (2022). Strategies for improving peptide stability and delivery. *Pharmaceuticals, 15*(10), 1283. https://doi.org/10.3390/ph15101283

Alsedfy, M. Y., Ebnalwaled, A. A., Moustafa, M., & Said, A. H. (2024). Investigating the binding affinity, molecular dynamics, and ADMET properties of curcumin-IONPs as a mucoadhesive bioavailable oral treatment for iron deficiency anemia. *Scientific Reports, 14*(1), 22027. https://doi.org/10.1038/s41598-024-72577-8

Angkoso, H., & Kekalih, A. (2022). Prognostic factors for mortality of pediatric burn injury in a national tertiary referral center. *The New Ropanasuri Journal of Surgery*, *7*(2). https://doi.org/10.7454/nrjs.v7i2.1134

Aisyah, S., Yulia, R., Saputro, I., & Herawati, F. (2018). Evaluation of antibiotic use and bacterial profile in burn unit patients at the dr. Soetomo general hospital. *Annals of Burns and Fire Disasters, 31*(3), 194. https://pmc.ncbi.nlm.nih.gov/articles/PMC6367852/

Bondos, S. E., Dunker, A. K., & Uversky, V. N. (2022). Intrinsically disordered proteins play diverse roles in cell signaling. *Cell Communication and Signaling, 20*(1), 20. https://doi.org/10.1186/s12964-022-00821-7

Burgess, M., Valdera, F., Varon, D., Kankuri, E., & Nuutila, K. (2022). The immune and regenerative response to burn injury. *Cells, 11*(19), 3073. https://doi.org/10.3390/cells11193073

Cabral, M. B., Dela-Cruz, C. J., Sato, Y., Oyong, G., Rempillo, O., Galvez, M. C., & Vallar, E. (2022). *In silico* approach in the evaluation of pro-inflammatory potential of polycyclic aromatic hydrocarbons and volatile organic compounds through binding affinity to the human toll-like receptor 4. *International Journal of Environmental Research and Public Health, 19*(14), 8360. https://doi.org/10.3390/ijerph19148360

Chen, H., Wubbolts, R. W., Haagsman, H. P., & Veldhuizen, E. J. A. (2018). Inhibition and eradication of *Pseudomonas aeruginosa* biofilms by host defence peptides. *Scientific Reports, 8*(1). https://doi.org/10.1038/s41598-018-28842-8

Chung, J., Eisha, S., Park, S., Morris, A. J., & Martin, I. (2023). How three self-secreted biofilm exopolysaccharides of *Pseudomonas aeruginosa*, psl, pel, and alginate, can each be exploited for

antibiotic adjuvant effects in cystic fibrosis lung infection. *International Journal of Molecular Sciences, 24*(10), 8709. https://doi.org/10.3390/ijms24108709

Dou, Y., Huan, J., Guo, F., Zhou, Z., & Shi, Y. (2017). *Pseudomonas aeruginosa* prevalence, antibiotic resistance and antimicrobial use in Chinese burn wards from 2007 to 2014. *The Journal of International Medical Research, 45*(3), 1124–1137. https://doi.org/10.1177/0300060517703573

Duarte-Mata, D. I., & Salinas-Carmona, M. C. (2023). Antimicrobial peptides´ immune modulation role in intracellular bacterial infection. *Frontiers in Immunology, 14*, 1119574. https://doi.org/10.3389/fimmu.2023.1119574

Dzurová, L., Holásková, E., Pospíšilová, H., Schneider Rauber, G., & Frébortová, J. (2024). Cathelicidins: Opportunities and challenges in skin therapeutics and clinical translation. *Antibiotics, 14*(1), 1. https://doi.org/10.3390/antibiotics14010001

Farhana, A., & Khan, Y. S. (2023, April 17). *Biochemistry, lipopolysaccharide*. PubMed; StatPearls Publishing. https://www.ncbi.nlm.nih.gov/books/NBK554414/

Franklin, M. J., Nivens, D. E., Weadge, J. T., & Howell, P. L. (2011). Biosynthesis of the *Pseudomonas aeruginosa* extracellular polysaccharides, alginate, Pel, and Psl. *Frontiers in Microbiology, 2*, 167. https://doi.org/10.3389/fmicb.2011.00167

Ghosh, A., Jayaraman, N., & Chatterji, D. (2020). Small-molecule inhibition of bacterial biofilm. *ACS Omega, 5*(7), 3108-3115. https://doi.org/10.1021/acsomega.9b03695

Gonzalez, M. R., Fleuchot, B., Lauciello, L., Jafari, P., Applegate, L. A., Raffoul, W., Que, Y. A., & Perron, K. (2016). Effect of human burn wound exudate on *Pseudomonas aeruginosa* virulence. *mSphere, 1*(2), e00111–15. https://doi.org/10.1128/mSphere.00111-15

Greenhalgh, D. G. (2019). Management of burns. *The New England Journal of Medicine, 380*(24), 2349–2359. https://doi.org/10.1056/NEJMra1807442

Gyawali, B., Ramakrishna, K., & Dhamoon, A. S. (2019). Sepsis: The evolution in definition, pathophysiology, and management. *SAGE Open Medicine, 7*, 2050312119835043. https://doi.org/10.1177/2050312119835043

Hateet, R. R. (2021). Isolation and identification of some bacteria contemn in burn wounds in Misan, Iraq. *Archives of Razi Institute, 76*(6), 1665. https://doi.org/10.22092/ari.2021.356367.1833

Hughes, G., & Webber, M. A. (2017). Novel approaches to the treatment of bacterial biofilm infections. *British Journal of Pharmacology, 174*(14), 2237–2246. https://doi.org/10.1111/bph.13706

Huszczynski, S. M., Lam, J. S., & Khursigara, C. M. (2020). The role of *Pseudomonas aeruginosa* lipopolysaccharide in bacterial pathogenesis and physiology. *Pathogens, 9*(1), 6. https://doi.org/10.3390/pathogens9010006

Jeschke, M. G., van Baar, M. E., Choudhry, M. A., Chung, K. K., Gibran, N. S., & Logsetty, S. (2020). Burn injury. *Nature Reviews Disease Primers, 6*(1), 11. https://doi.org/10.1038/s41572-020-0145-5

Keikhosravani, P., Jahanmard, F., Bollen, T., Nazmi, K., A. Veldhuizen, E. J., Gonugunta, P., Anusuyadevi, P. R., Vogely, C., Bikker, F. J., Taheri, P., Weinans, H., & Yavari, S. A. (2023). Antibacterial CATH-2 peptide coating to prevent bone implant-related infection. *Advanced Materials Technologies, 8*(18), 2300500. https://doi.org/10.1002/admt.202300500

Kulkarni, N. N., O'Neill, A. M., Dokoshi, T., Luo, E. W. C., Wong, G. C. L., & Gallo, R. L. (2021). Sequence determinants in the cathelicidin LL-37 that promote inflammation *via* presentation of RNA to scavenger receptors. *The Journal of Biological Chemistry, 297*(1), 100828. https://doi.org/10.1016/j.jbc.2021.100828

Lee, E., & Anjum, F. (2023). *Staphylococcus epidermidis infection*. PubMed; StatPearls Publishing. https://www.ncbi.nlm.nih.gov/books/NBK563240/

Lin, M., Chen, S., Chen, Y., Gao, Q. (2025). Exploring the molecular mechanism of budesonide enteric capsules in the treatment of IgA nephropathy based on bioinformatics. *Scientific Reports, 15*, 30795. https://doi.org/10.1038/s41598-025-16380-z

Melamed, J., & Brockhausen, I. (2021). Biosynthesis of bacterial polysaccharides. *Comprehensive Glycoscience, 3*, 143–178. https://doi.org/10.1016/B978-0-12-819475-1.00097-3

Muntaha, S. T., Rakha, A., Rasheed, H., Fatima, I., Butt, M. S., Abdi, G., & Aadil, R. M. (2025). Polyphenol-protein particles: A nutraceutical breakthrough in nutrition and food science. *Journal of Agriculture and Food Research, 101641*. https://doi.org/10.1016/j.jafr.2025.101641

Pradhan, N., & Sharma, K. (2014). Understanding Ubl-Rpn1 intermolecular interaction. *Journal of Advanced Pharmaceutical Science and Technology, 1*(3), 1–11. https://doi.org/10.14302/issn.2328-0182.japst-13-288

Preda, V. G., & Săndulescu, O. (2019). Communication is the key: Biofilms, quorum sensing, formation and prevention. *Discoveries*, *7*(3), e10. https://pmc.ncbi.nlm.nih.gov/articles/PMC7086079/

Radzikowska-Büchner, E., Łopuszyńska, I., Flieger, W., Tobiasz, M., Maciejewski, R., & Flieger, J. (2023). An overview of recent developments in the management of burn injuries. *International Journal of Molecular Sciences, 24*(22), 16357. https://doi.org/10.3390/ijms242216357

Ridyard, K. E., & Overhage, J. (2021). The potential of human peptide LL-37 as an antimicrobial and anti-biofilm agent. *Antibiotics, 10*(6), 650. https://doi.org/10.3390/antibiotics10060650

Ruff, K. M., & Pappu, R. V. (2021). AlphaFold and implications for intrinsically disordered proteins. *Journal of Molecular Biology, 433*(20), 167208. http://dx.doi.org/10.1016/j.jmb.2021.167208

Sancho-Vaello, E., Gil-Carton, D., François, P., Bonetti, J., Kreir, M., Pothula, K. R., Kleinekathöfer, U., & Zeth, K. (2020). The structure of the antimicrobial human cathelicidin LL-37 shows oligomerization and channel formation in the presence of membrane mimics. *Scientific Reports, 10*, 17356. https://doi.org/10.1038/s41598-020-74401-5

Salam, M. A., Al-Amin, M. Y., Salam, M. T., Pawar, J. S., Akhter, N., Rabaan, A. A., & A Alqumber, M. A. (2023). Antimicrobial resistance: A growing serious threat for global public health. *Healthcare, 11*(13), 1946. https://doi.org/10.3390/healthcare11131946

Sarkar, A., Concilio, S., Sessa, L., Marrafino, F., & Piotto, S. (2023). Advancements and novel approaches in modified AutoDock Vina algorithms for enhanced molecular docking. *Results in Chemistry, 7*, 101319. https://doi.org/10.1016/j.rechem.2024.101319

Scheenstra, M. R., van den Belt, M., Tjeerdsma-van Bokhoven, J. L. M., Schneider, V. A. F., Ordonez, S. R., van Dijk, A., Veldhuizen, E. J. A., & Haagsman, H. P. (2019). Cathelicidins PMAP-36, LL-37 and CATH-2 are similar peptides with different modes of action. *Scientific Reports, 9*(1), 4780. https://doi.org/10.1038/s41598-019-41246-6

Scheenstra, M. R., van Harten, R. M., Veldhuizen, E. J. A., Haagsman, H. P., & Coorens, M. (2020). Cathelicidins modulate TLR-activation and inflammation. *Frontiers in Immunology, 11*, 1137. https://doi.org/10.3389/fimmu.2020.01137

Schneider, V. A., Coorens, M., Ordonez, S. R., Tjeerdsma-van Bokhoven, J. L., Posthuma, G., van Dijk, A., Haagsman, H. P., & Veldhuizen, E. J. (2016). Imaging the antimicrobial mechanism(s) of cathelicidin-2. *Scientific Reports, 6*(1), 32948. https://doi.org/10.1038/srep32948

Sharma, S., Mohler, J., Mahajan, S. D., Schwartz, S. A., Bruggemann, L., & Aalinkeel, R. (2023). Microbial biofilm: A review on formation, infection, antibiotic resistance, control measures, and innovative treatment. *Microorganisms, 11*(6), 1614. https://doi.org/10.3390/microorganisms11061614

Soleymanzadeh-Moghadam, S., Azimi, L., Amani, L., Lari, A. R., Alinejad, F., & Lari, A. R. (2015). Analysis of antibiotic consumption in burn patients. *GMS Hygiene and Infection Control, 10*, Doc09. https://doi.org/10.3205/dgkh000252

Tasleem, S., Siddiqui, A. I., Zuberi, M. A. W., Tariq, H., Abdullah, M., Hameed, A., Aijaz, A., Shah, H. H., Hussain, M. S., & Oduoye, M. O. (2024). Mortality patterns and risk factors in burn patients: A cross-sectional study from Pakistan. *Burns Open, 8*(1), 13–18. https://doi.org/10.1016/j.burnso.2023.11.003

Terwilliger, T. C., Liebschner, D., Croll, T. I., Williams, C. J., McCoy, A. J., Poon, B. K., Afonine, P. V., Oeffner, R. D., Richardson, J. S., Read, R. J., & Adams, P. D. (2024). AlphaFold predictions are valuable hypotheses and accelerate but do not replace experimental structure determination. *Nature Methods, 21*(1), 110–116. https://doi.org/10.1038/s41592-023-02087-4

Thakur, B., Arora, K., Gupta, A., & Guptasarma, P. (2020). Mechanism of bacterial adhesion and embedment in a DNA biofilm matrix: Evidence that binding of outer membrane lipopolysaccharide (LPS) to HU is key. *bioRxiv*. https://doi.org/10.1101/2020.10.20.346890

van Harten, R. M., Van Woudenbergh, E., Van Dijk, A., & Haagsman, H. P. (2018). Cathelicidins: immunomodulatory antimicrobials. *Vaccines, 6*(3), 63. https://doi.org/10.3390/vaccines6030063

Varadi, M., Anyango, S., Deshpande, M., Nair, S., Natassia, C., Yordanova, G., Yuan, D., Stroe, O., Wood, G., Laydon, A., Žídek, A., Green, T., Tunyasuvunakool, K., Petersen, S., Jumper, J., Clancy, E., Green, R., Vora, A., Lutfi, M., ... Velankar, S. (2022). AlphaFold protein structure database: Massively expanding the structural coverage of protein-sequence space with high-accuracy models. *Nucleic Acids Research, 50*(D1), D439–D444. https://doi.org/10.1093/nar/gkab1061

Varela, M. F., Stephen, J., Lekshmi, M., Ojha, M., Wenzel, N., Sanford, L. M., Hernandez, A. J., Parvathi, A., & Kumar, S. H. (2021). Bacterial resistance to antimicrobial agents. *Antibiotics, 10*(5), 593. https://doi.org/10.3390/antibiotics10050593

Vittorio, S., Lunghini, F., Morerio, P., Gadioli, D., Orlandini, S., Silva, P., Martinovic, J., Pedretti, A., Bonanni, D., del Bue, A.,Palermo, G., Vistoli, G., & Beccari, A. R. (2024). Addressing docking pose selection with structure-based deep learning: Recent advances, challenges and opportunities. *Computational and Structural Biotechnology Journal, 23*, 2141–2151. https://doi.org/10.1016/j.csbj.2024.05.024

Wang, G. (2008). Structures of human host defense cathelicidin LL-37 and its smallest antimicrobial peptide KR-12 in lipid micelles. *Journal of Biological Chemistry, 283*(47), 32637–32643. https://doi.org/10.1074/jbc.M805533200

Wardhana, A., Basuki, A., Prameswara, A. D. H., Rizkita, D. N., Andarie, A. A., & Canintika, A. F. (2017). The epidemiology of burns in Indonesia's national referral burn center from 2013 to 2015. *Burns Open, 1*(2), 67–73. https://doi.org/10.1016/j.burnso.2017.08.002

Whitfield, C., Williams, D. M., & Kelly, S. D. (2020). Lipopolysaccharide O-antigens-bacterial glycans made to measure. *The Journal of Biological Chemistry, 295*(31), 10593–10609. https://doi.org/10.1074/jbc.REV120.009402

World Health Organization. (2023). Burns. https://www.who.int/news-room/fact-sheets/detail/burns

Xiao, Q., Luo, Y., Shi, W., Lu, Y., Xiong, R., Wu, X., Huang, H., Zhao, C., Zeng, J., & Chen, C. (2022). The effects of LL-37 on virulence factors related to the quorum sensing system of *Pseudomonas aeruginosa*. *Annals of Translational Medicine, 10*(6), 284. https://doi.org/10.21037/atm-22-617

Yasir, M., Willcox, M., & Dutta, D. (2018). Action of antimicrobial peptides against bacterial biofilms. *Materials, 11*(12), 2468. https://doi.org/10.3390/ma11122468

Zhang, Y., Yu, C., Shan, T., Chen, Y., Wang, Y., Xie, M., Li, T., Yang, Z., & Zhong, H. (2022). Solvent-assisted conformational interconversion of an organic semiconductor with multiple non-covalent interactions. *Cell Reports Physical Science, 3*(3). https://doi.org/10.1016/j.xcrp.2022.100765

Żwierełło, W., Piorun, K., Skórka-Majewicz, M., Maruszewska, A., Antoniewski, J., & Gutowska, I. (2023). Burns: Classification, pathophysiology, and treatment: A review. *International Journal of Molecular Sciences, 24*(4), 3749. https://doi.org/10.3390/ijms24043749